

Proper orthogonal decomposition of an axisymmetric turbulent wake behind a disk

Peter B. V. Johansson^{a)} and William K. George

*Department of Thermo and Fluid Dynamics, Chalmers University of Technology,
SE-412 96 Gothenburg, Sweden*

Scott H. Woodward

Department of Mechanical and Aerospace Engineering, University at Buffalo, Buffalo, New York 14260

(Received 24 September 2001; accepted 14 March 2002; published 5 June 2002)

A proper orthogonal decomposition (POD) study of the axisymmetric turbulent wake behind a disk has been performed using multipoint hot-wire data. The Reynolds number based on the free stream velocity and disk diameter was kept constant at 28 000. The investigated region spanned from 10 to 50 disk diameters downstream. The hot-wire data were obtained using two rakes: a seven wire fixed array and a six wire array azimuthally traversable to span the cross section of the flow in increments of 15°. The instantaneous streamwise velocity component data were Fourier transformed in time and decomposed in Fourier series in the azimuthal direction to form the kernel for the POD. For all downstream positions, two distinct peaks were found in the first eigenspectrum: one at azimuthal mode 2 at near zero frequency, and another at azimuthal mode 1 at a fixed Strouhal number (fd/U_∞) of 0.126. Both peaks decrease in magnitude as the flow evolves downstream, but the peak at the Strouhal number 0.126 decreases more rapidly than the one at near-zero frequency, leaving the latter to eventually dominate. Because of this evolution, the eigenvalues integrated over frequency show an azimuthal mode-1 dominance at $x/D=10$ and a mode-2 dominance by $x/D=50$. The results are compared to those recently obtained in the axisymmetric far jet, and the results of previous wake investigations. © 2002 American Institute of Physics. [DOI: 10.1063/1.1476301]

I. INTRODUCTION

The turbulent wake behind an axisymmetric object such as a disk or a sphere has been under investigation for almost a century. This flow is of considerable practical importance because of its close relation to many aero- and hydrodynamic applications. In addition, it is of fundamental importance since it is one of the few shear flows where the local turbulence Reynolds number decreases as the flow evolves. Also, the equations of motion governing the axisymmetric wake contain all of the important dynamical terms for turbulent flow away from surfaces. Hence the data from this flow form an important database for developing turbulence models of all types.

Early experiments on the fundamental features of this flow focused on the far wake. One pioneering study was made by Hwang and Baldwin,¹ who measured turbulence intensities and wake growth for a large span of downstream locations, $x/d=5$ to $x/d\approx 900$. Because the high demands on equipment could not be met at this time, there was severe scatter in their data; and they even reported difficulties in reproducing their own results on a day-to-day basis. More recently, researchers have primarily focused on the early development of the wake or on its stability.²⁻⁵ An exception was the careful far wake measurements of Cannon⁶ and Cannon, Champagne and Glezer,⁷ who found very different results depending on the wake generator used. Intriguingly,

they were unable to resolve satisfactorily whether the classical similarity theory applied, a subject addressed in detail by Johansson and George.⁸

The large scale, “coherent” features of this flow have been investigated by means of flow visualization, multipoint, phase averaging and conditional sampling techniques.^{7,9-15} These findings have contributed to our understanding of the process of vortex formation behind the generator. There have also been discussions about the randomness and antiphase characteristics of vortex structures behind axisymmetric bodies. Most interestingly in the context of the present work, Fuchs *et al.*¹⁰ used two hot wires to measure cross spectra at a single radius of the near wake. This radius varied from $r/D=0.75$ at $x/D=3$ to $r/D=0.83$ at $x/D=9$. The angular separation of the probes was varied in steps of 30°, and the measured cross spectra were decomposed into Fourier series in the azimuthal direction. The azimuthal modal content was then studied at the frequencies that were found to be eventful. At $x/D=9$, Fuchs *et al.*¹⁰ found a strong azimuthal mode $m=1$ peak in the coherence spectrum at the natural Strouhal number $S_n=f_n D/U_\infty=0.135$. They also found a distinct peak at azimuthal mode $m=2$ at a near-zero frequency ($S_2=0.005$; Figs. 9–11 of their paper). There was no suggestion, however, that $m=2$ was the dominant mode, nor is it found to be so in our study until much further downstream (Fig. 7 in this paper).

The first of these results was confirmed by Berger *et al.*,¹¹ who also found the $m=1$ peak, but they did not report any $m=2$ peak. This was a curious omission, since it

^{a)}Electronic mail: jope@tfd.chalmers.se

is clearly present at low frequency in their coherence spectra, Fig. 4 ($x/D=9$, $r/D=0.83$, disk at rest) and Fig. 6 ($x/D=6$, $r/D=0.83$, nutating disk) of their paper, exactly as noted by Fuchs *et al.*¹⁰ Instead, they focus on the $m=1$, $S_n=0.135$ peak, and interpret this near wake result as a helical vortex structure. From here on, nothing is mentioned in the literature about the occurrence of azimuthal mode $m=2$, and it has been presumed until now that azimuthal mode $m=1$ is the most dominant. This is also the result obtained from the linear parallel stability analysis of Monkewitz,⁴ and the non-linear dynamical systems approach by Ghidersa and Dušek.⁵

Because of the small velocity deficit, the very low turbulence intensities, and the slow decay of the velocity deficit downstream, the far axisymmetric wake still is at the threshold of what is possible to measure using even the best wind tunnels and the most stable low-noise anemometer equipment. The work reported here is part of a continuing effort to measure and understand this flow. In the present work, the evolution of the wake is studied using a so-called “slice” version of the proper orthogonal decomposition (POD) technique. The term “slice POD” refers to decomposing the flow field at fixed downstream locations in the remaining cross-stream coordinates. This method has been previously applied to the jet mixing layer^{16–18} and far jet¹⁹ to quantify the energetics of the POD modes.

II. EXPERIMENTAL SETUP

The experiments were performed in the low-turbulence wind tunnel at Chalmers University of Technology, Gothenburg, Sweden. The free-stream streamwise turbulence intensity over the span of velocities related to this work was less than 0.03%. The measuring cross section in the tunnel is $1.80 \times 1.25 \text{ m}^2$ and the downstream length is 3.00 m. Special attention was made to avoid flow blockage by the wake generator. The disk used had a diameter of 28 mm, and was suspended with four pairs of wires, each with the diameter 0.2 mm. The total area ratio between the object and tunnel cross section was less than 0.03%. The tunnel velocity was kept constant at 15 m/s during the experiment, resulting in a Reynolds number based on the free stream velocity and disk diameter of 28 000.

A total number of 13 hot wires were used in the two arrays as shown in Fig. 1. The arrays were used in the same manner as Glauser and George¹⁷ to obtain the two-point velocity cross spectra for all combinations of locations shown in Fig. 2. The measurement grid was chosen following Glauser and George,²⁰ so as to provide an optimum resolution to apply the POD. The upper array of probes was movable, and traversed from a 15° separation up to 180° with 15° increments in $\Delta\theta$, see Fig. 2. Each hot-wire probe is numbered and marked by a circle. The angle separation $\Delta\theta=135^\circ$ could not be measured directly, since the movable probe rake caught the wake of the suspending wires. Instead, measurements at the angles 130° and 140° were used to estimate this position. In all, half the cross section of the wake at a fixed downstream position was scanned, and pairs of instantaneous velocity cross spectra for a fixed angle separation computed.

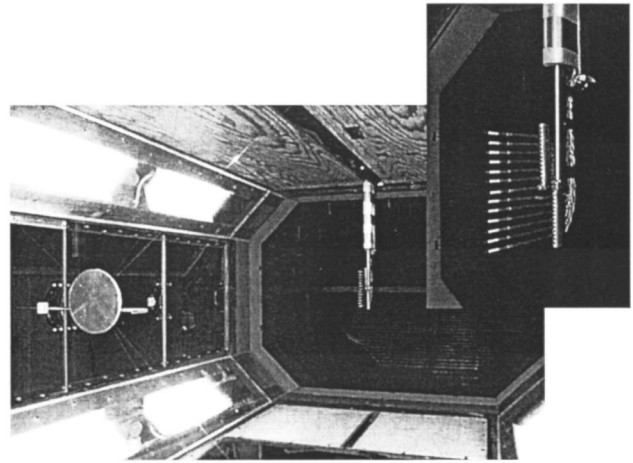


FIG. 1. The probe array and disk in the Chalmers wind tunnel.

Note that the cross spectra corresponding to the remaining half-plane were available from the azimuthal symmetry of the flow.

Each single hot wire, 3 mm long and made of unplated $5 \mu\text{m}$ tungsten wire, was oriented to measure the streamwise component of the velocity. The probes were connected to an AN2000 Constant Temperature Anemometer (CTA) system, and sampled with an IO Tech Wavebook 516 16 bit sample and hold A/D converter. The data were low-pass filtered at 2 kHz and sampled at 6 kHz for all configurations, substantially higher than required by the temporal Nyquist criterion. Measurements were made simultaneously at all 13 positions. Each block had 8192 samples, and a total of 300 blocks of data was taken per probe for each angular probe location, ensuring a variability of less than 6% for the cross spectra used in the POD.

III. PROPER ORTHOGONAL DECOMPOSITION

The POD, a well-known mathematical technique which appears under several other names as well (e.g., singular value decomposition, Karhunen–Loève decomposition, principal value analysis), was introduced to the study of turbulence by Lumley.²¹ The mathematical aspects are very well

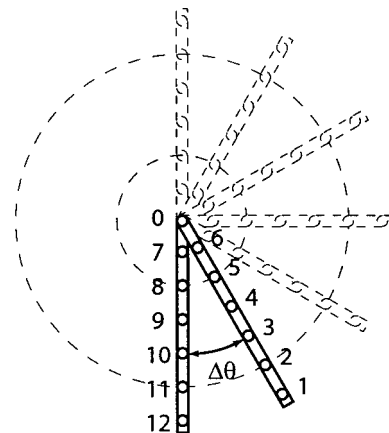


FIG. 2. The traversing scheme, shown in 30° increments in $\Delta\theta$ for simplicity.

described elsewhere (e.g., Refs. 18, 19, 22, 23), so we will very briefly point out only the most essential features and focus on the actual procedure used in this work to analyze the data.

The core of the POD is a projection of the velocity field, u_i , into a coordinate system, ϕ_i , optimal in terms of energy, i.e., maximizing

$$\frac{\langle (u_i, \phi_i)^2 \rangle}{\|\phi_i\|} = \lambda. \quad (1)$$

This can be shown by calculus of variations to result in the following integral equation:

$$\int_D R_{i,j}(\cdot, \cdot') \phi_j(\cdot') r' d(\cdot') = \lambda \phi_i(\cdot), \quad (2)$$

where the kernel, $R_{i,j} = \langle u_i(\cdot) u_j(\cdot') \rangle$, is the two-point velocity correlation tensor and (\cdot) represents the spatial coordinates and time, or a subset of these.

If the field has finite total energy, Hilbert–Schmidt theory assures that the solution exists and consists of a denumerable, infinite, set of eigenvalues, $\lambda^{(n)}$, and corresponding eigenfunctions, $\phi_i^{(n)}$. For an axisymmetric shear flow such as a jet or a wake, this is true in the radial direction at a single downstream location, hence the term “slice POD.”

The modes are ordered so that the first mode contains most of the energy, and the relation between the kinetic energy and the eigenvalues is given by

$$E = \int_D u_i(\cdot) u_i^*(\cdot) d(\cdot) = \sum \lambda^{(n)}. \quad (3)$$

The axisymmetric wake in question is *stationary* in time and *periodic* in the azimuthal direction. Therefore, the Hilbert–Schmidt theory does not apply, but the POD modes in these directions can be shown to be Fourier modes, see George.²⁴

If only the streamwise velocity component at a fixed downstream location is considered (i.e., $i = j = 1$), the following integral equation(s) must be solved:

$$\begin{aligned} \int_0^\infty B_{1,1}(m, f, r, r'; x) \psi_1^{(n)}(m, f, r'; x) r' dr' \\ = \lambda^{(n)}(m, f; x) \psi_1^{(n)}(m, f, r; x), \end{aligned} \quad (4)$$

where $B_{1,1}(m, f, r, r'; x)$ is the two-point velocity correlation Fourier transformed in time and expanded in Fourier series in the azimuthal direction, the $\psi_1^{(n)}(m, f, r; x)$ are the eigenfunctions, and $\lambda^{(n)}(m, f; x)$ the corresponding eigenspectra.

In practice, the following steps are taken (following Glauser and George¹⁷):

- (1) Measurement of the instantaneous velocity at two points.
- (2) Fourier transformation in time and computation of the cross spectrum.
- (3) Repetition of (1) and (2) for many pairs of points.
- (4) Expansion of the cross spectra obtained in (2) in Fourier series in the azimuthal direction.
- (5) Solution of the remaining eigenvalue problem (in the radial direction), Eq. (4) for each frequency and azimuthal mode number.

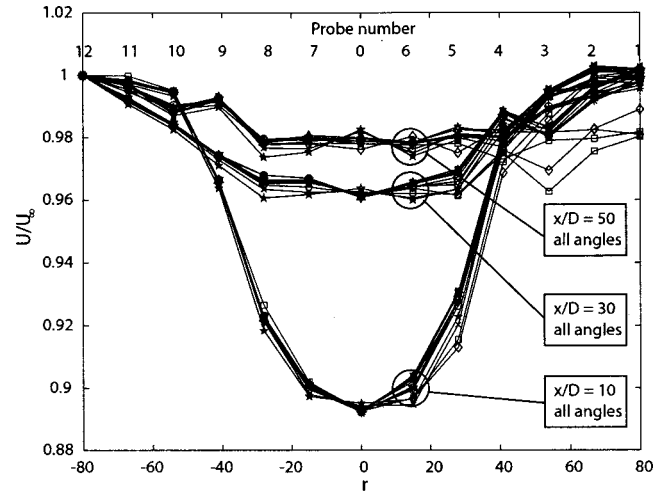


FIG. 3. Mean velocity profiles, U/U_∞ , $x/D = 10, 30, \text{ and } 50$. $\Delta\theta = 15^\circ, 30^\circ, \dots, 180^\circ$.

Note that this procedure is different than that implemented by Citriniti and George¹⁸ and Gamard *et al.*,¹⁹ since in their experiments the velocity at all grid points was obtained simultaneously using a 138-wire probe. Here, only pairs of points were available for the given rake positions, so the procedure had to be repeated as the movable rake was rotated through the entire 180° . This is exactly the procedure used by Glauser and George¹⁷ in an earlier jet mixing layer study.

IV. STATISTICAL RESULTS

In order to ensure the reliability of the data before performing the POD, first- and second-order statistical properties were analyzed. Mean velocity profiles, scaled by the tunnel velocity, U_∞ , for the three downstream locations are shown in Fig. 3. The velocity deficit ranges from around 11% of the free-stream velocity at $x/D = 10$, to about 2% at $x/D = 50$. The left-hand side of the plot (negative r) corresponds to the fixed array of probes, and the right-hand side (positive r) the movable. These clearly show one of the main difficulties measuring this flow using hot wires: the velocity deficit is very small, and thus extremely sensitive to the accuracy of the measuring device. These multipoint measurements extended typically over 8–10 h because of the many cross spectra needed ($7 \times 7 \times 13$), thus the data are very much affected by any drift in the anemometers (primarily associated with thermal instability of the dc offset amplifier). The thermal drift problems with the CTA usually shows up as a calibration error, and is probably the reason most previous researchers interested in the mean profiles have used Pitot-tubes. A separate contribution to the systematic variation in the data is the problem of aligning the arrays of probes to the wake center. Unlike earlier investigations which used only at most a single linear rake, these errors are more obvious here because of the movable array of probes (i.e., positive r), and show up as an increased spread of data. Nevertheless, the overall quality of the data compares favorably with those of Cannon,⁶ for example. The mean velocity profile at $x/D = 50$ around the angle 135° is also clearly affected by inter-

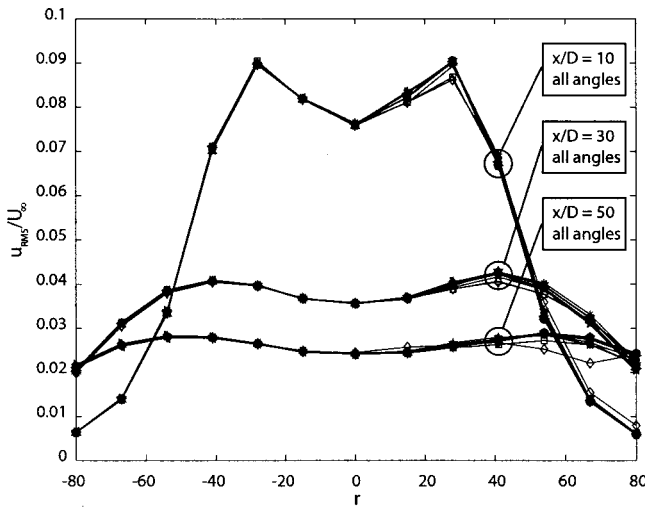


FIG. 4. Turbulence intensity profiles, $x/D=10, 30,$ and 50 . $\Delta\theta=15^\circ, 30^\circ, \dots, 180^\circ$.

ference from the wakes of the wires supporting the disk. The data were replaced in the POD calculations by the average of the spectral values at 130° and 140° .

Root mean square velocity profiles were computed and a plot covering all angles and downstream positions is reproduced in Fig. 4. The turbulence intensities, $\sqrt{u^2}/U_\infty$, are very small, from 9% at $x/D=10$ to below 3% at $x/D=50$. But here, the situation is entirely different from that for the mean velocity; the thermal drift in the anemometers is clearly not affecting the fluctuating velocities. This is because even though the anemometer output voltage was drifting slowly (due to the dc offset amplifier), the slope of the calibration curve near the tunnel velocity at which the data were obtained remained nearly constant. (This was confirmed by repeated recalibrations during the experiment.) Thus the fluctuating velocities for these very low turbulence intensities are correctly measured. The consequence of not being able to exactly center the probe rake can still be seen in the right-hand side of the plots. As with the mean velocity profiles at $x/D=50$, the support wire wake has grown enough so that the results from angle 135° are affected by it.

Power spectral densities (PSDs) were computed for all downstream positions as well as rotations of the movable rake. Figure 5 shows the PSDs at $x/D=10, 30,$ and 50 , respectively, for the probe rake separation $\Delta\theta=180^\circ$. All PSDs off the center of the wake show a prominent peak at 67 Hz, corresponding to a Strouhal number ($St=fd/U_\infty$) of 0.126. This is consistent with Strouhal number measured by Miao *et al.*¹³ in the near wake. The magnitude of this peak decreases with increased downstream position, but is still clearly visible at $x/D=50$. From the absence of this peak in the center of the wake, one can immediately infer that this type of motion, a very dominant feature of the PSD, cannot be related to an azimuthal mode-0 motion.

V. POD RESULTS

A. Eigenspectra, $\lambda^{(n)}(m, f; x)$

Eigenspectra were computed for the three downstream locations by solving Eq. (4) to obtain the distribution

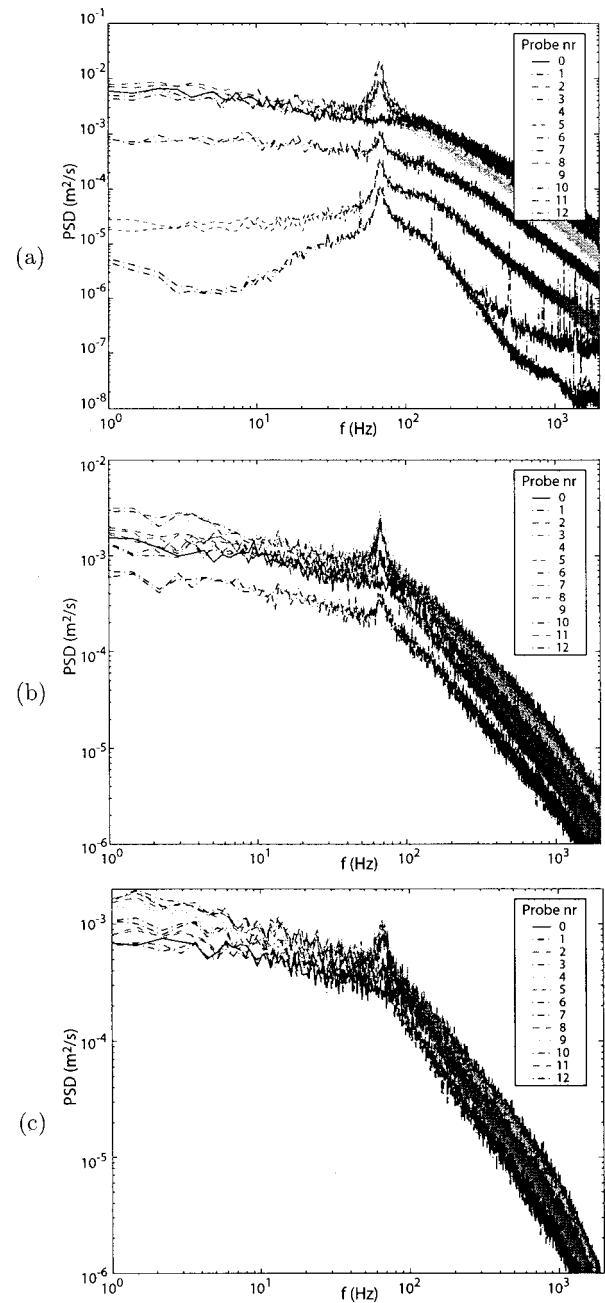


FIG. 5. Power spectral densities, $\Delta\theta=180^\circ$ for all probes at different downstream positions: (a) $x/D=10$, (b) 30, and (c) 50.

$\lambda^{(n)}(m, f; x)$. Even this simple result from the POD provides a large amount of information regarding the overall energy distribution in the flow, and the results can be viewed from many perspectives. Several of these will be presented in the following.

The eigenspectra, $\lambda^{(n)}(m, f; x)$, are representations of how the energy is distributed as a function of azimuthal mode number, m , and frequency, f , at a given downstream position, x . Therefore their evolution shows how the main characteristics of the flow evolve. Three-dimensional and contour plots of the eigenspectra for the first POD mode ($n=1$) are presented in Fig. 6 for the three downstream positions covered in this study. The three pictures are strikingly similar and the general features do not evolve with down-

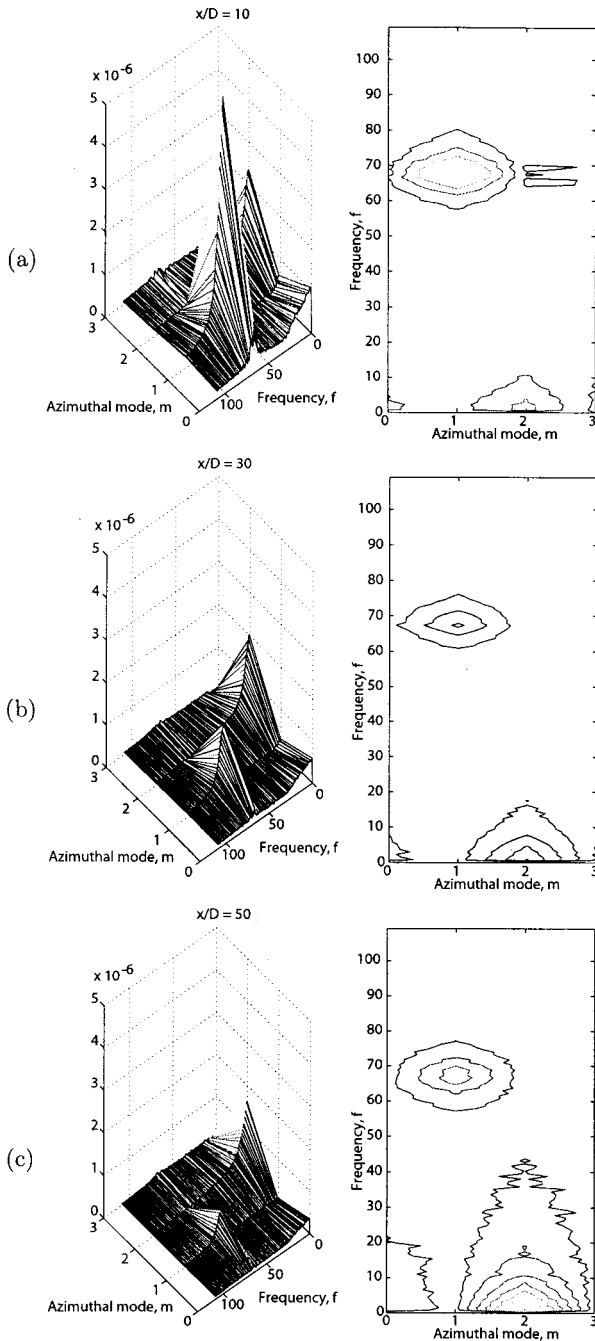


FIG. 6. Eigenspectrum function of azimuthal mode number (m) and frequency (f) at different downstream positions: (a) $x/D=10$, (b) 30, and (c) 50.

stream distance. The energy is concentrated around two separate peaks in the f - m plane. One is at near-zero frequency for azimuthal mode $m=2$ and the other for azimuthal mode $m=1$ at a higher frequency, 67 Hz. This second peak for $m=1$ corresponds to a Strouhal number of 0.126. This Strouhal number does not change with downstream position, and is exactly the same as the one detected in the PSDs off the wake center described in Sec. IV. The magnitude of these peaks decreases as the flow evolves. It is also clear that the peak at $m=1$ is largest at $x/D=10$, but decreases more rapidly than the $m=2$ peak, leaving the latter the largest by $x/D=50$. From these pictures, it is not at all clear what role

$m=0$ plays. It does not seem to be directly connected to a specific frequency.

Our results at $x/D=10$ can be compared to those of Fuchs *et al.*¹⁰ They did not use the POD, but measured cross spectra only at a single radius of the near wake as noted in Sec. I. At $x/D=3$, they found a strong azimuthal mode $m=1$ peak in the coherence spectrum at the natural Strouhal number $S_1=f_n D/U_\infty=0.135$. Their Reynolds number was 50 000, which explains the higher Strouhal number than in the present work where $Re=28\,000$, but fully consistent with the results of Miau *et al.*¹³ Higher azimuthal modes were all of the same order and small compared to the dominating one. At $x/D=9$, however, the $m=1$ peak was still dominant (at $S_1=0.135$), but they also found a distinct peak at azimuthal mode $m=2$ at a near-zero frequency ($S_2=0.005$; Figs. 9–11 of their paper). Their Fig. 9 also contains data of Roberts,⁹ which agree very well. These results are consistent with our findings at $x/D=10$ as seen in Fig. 6(a); namely that the largest peak in $\lambda^{(1)}$ is at $m=1$, $f=67$ Hz, whereas the peak at $m=2$, $f\approx 1$ Hz is smaller.

Our findings that mode 2 comes to dominate farther downstream appear to be new. These cannot yet be corroborated by the measurements of others, since none exist beyond those cited earlier. And none exist at all beyond $x/D=10$.

B. Eigenspectra integrated over frequency, $\xi^{(n)}(m;x)$

The eigenspectra can be integrated over frequency to illustrate another key property of the POD, its ability to show how the kinetic energy of the flow is distributed among the various azimuthal modes. To visualize the energy distribution per azimuthal mode number, m , we computed for each downstream position the quantity $\xi^{(n)}(m;x)$ where

$$\xi^{(n)}(m;x) = \frac{\int_f \lambda(m,f;x) df}{\sum_m \int_f \lambda(m,f;x) df}. \quad (5)$$

Here, the denominator is the total kinetic energy, as defined in Eq. (3). The resulting normalized eigenspectra, $\xi^{(n)}(m;x)$ are plotted in Fig. 7. Since the flow field is homogeneous in time (stationary) as well as in the azimuthal direction (periodic), this immediately imposes that the eigenspectrum, $\lambda^{(n)}(m,f;x)$, is symmetric with respect to these directions; i.e., $\lambda^{(n)}(m,f;x) = \lambda^{(n)}(-m,-f;x)$ (see Lumley²¹). When integrating over frequency, to obtain $\xi^{(n)}(m;x)$ according to Eq. (5), it is easy to show that $\xi^{(n)}(m;x)$ are also symmetric in m . Therefore, only positive m are shown in Fig. 7. From these, it is clear that at $x/D=10$, most of the energy lies in the azimuthal mode $m=1$, while at $x/D=50$, the most energetic azimuthal mode is $m=2$. At the intermediate position, both modes contain roughly the same fraction of the total energy. It is also clear that $m=0$ is the third most important azimuthal mode.

The overall behavior is strikingly similar to the results of Gamard *et al.*¹⁹ in the axisymmetric jet. In the jet, however, mode 2 becomes dominant by the end of the potential core ($x/D=6$), whereas here mode 2 does not dominate until $x/D=50$. This is, perhaps, related to the much higher turbulence intensity in the jet and its faster spreading rate. It might be noted that since $m=2$ also dominates at low frequencies

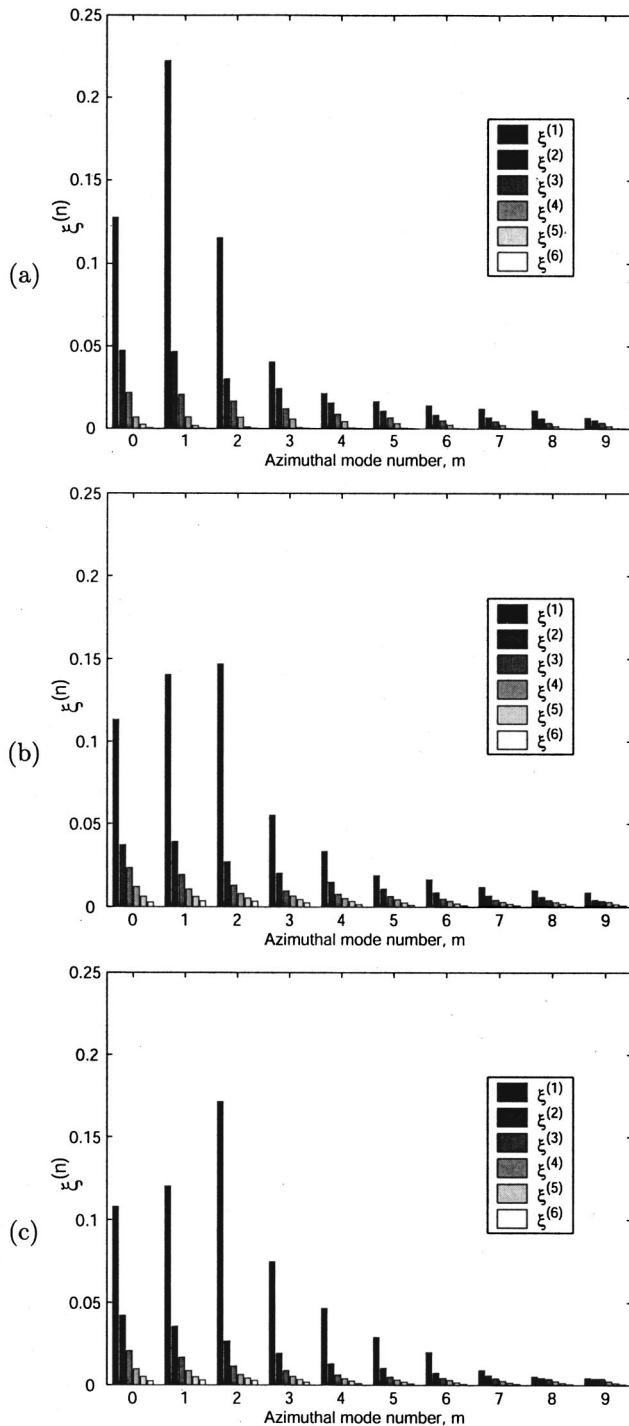


FIG. 7. Eigenspectra integrated over frequency as function of azimuthal mode number (m) at different downstream positions: (a) $x/D=10$, (b) 30, and (c) 50.

at large enough distance downstream in the jet of Gamard *et al.*,¹⁹ suggesting strongly that this is a natural feature of these very different flows, and not related to the facility.

VI. TAYLOR’S HYPOTHESIS AND INTERPRETATION OF FREQUENCY

So far in this paper, we have used the commonly adapted notation and presented our results concerning spectral con-

tent as a function of frequency, exactly as measured. In order to physically interpret the results, however, it is necessary to distinguish between spatial and temporal structures. In other words, we must sort out whether the observed “frequency” represents a true unsteadiness, or should be interpreted as a “wave number” using Taylor’s frozen field hypothesis.²⁵ In the far axisymmetric wake, the mean velocity deficit between the free stream and the center of the wake is small, varying from 11% at $x/D=10$ to 2% at $x/D=50$ as depicted in Fig. 3. Thus the mean velocity gradient is also very small, as is the turbulence intensity which is of the same order as the mean velocity differences (see Fig. 4). Thus the convection velocity can be approximated by the free stream (or equally well, the centerline) velocity.

These together, according to all the criteria in Lumley,²⁵ imply that for all but the very lowest frequencies, Taylor’s hypothesis is valid. Thus, the peak at 67 Hz must be interpreted as a frozen turbulence field that is convected by with the wavelength $\lambda = U_c/f = 0.22$ m. Even so, this “wavelength” can still arise from vortex shedding at the wake generator, since the disturbances generated there will be swept by the probe at approximately the free stream velocity, thereby yielding the same Strouhal frequency.

The situation is much less clear for mode 2 which has a near-zero frequency peak at approximately 1 Hz, since all the fundamental criteria for Taylor’s hypothesis are violated. Interpretation as a convected disturbance would suggest a disturbance 15 m long! This is clearly unphysical, and consistent with the breakdown of Taylor’s hypothesis at this low frequency. It is thus more likely that the mode-2 disturbance is related to a temporal variation of the wake itself. For example, one possibility might be a mode-2 distortion of the mean velocity, which itself precesses slowly. Clearly, multi-point measurements in the downstream and cross-stream directions simultaneously are required to sort this out.

VII. SUMMARY AND CONCLUSIONS

The axisymmetric turbulent wake behind a disk was studied using a “slice POD” for three fixed downstream cross sections of the flow. For all downstream positions, two distinct peaks were found in the first eigenspectrum: one at azimuthal mode $m=1$ at a fixed Strouhal number (fd/U_∞) of 0.126, and another at azimuthal mode $m=1$ at near-zero frequency. Both peaks decrease in magnitude as the flow evolves downstream, but the peak at $m=1$ decreases more rapidly than the one at $m=2$, leaving the latter to eventually dominate. Because of this evolution, the eigenvalues integrated over frequency show an azimuthal mode-1 dominance at $x/D=10$ and a mode-2 dominance by $x/D=50$. The $m=1$ peak can be associated with a “structure” of frozen turbulence that is convected downstream. The $m=2$ peak clearly is not a convected disturbance.

Despite being two different flows, the axisymmetric wake and the jet share many common features, in particular the mode-2 dominance asymptotically. It is reasonable to expect that the modes in these two flows can behave the same only if they are governed by similar equations, whatever they might be. By projecting the Navier–Stokes equations onto

the POD basis functions, Lumley²¹ showed that the linearized leading order equations reduce to the Orr–Sommerfeld equations (for the appropriate coordinate system). Thus it is reasonable to anticipate similarities between the POD decomposed measurements and linear stability analyses. Linear parallel stability analysis by Monkewitz⁴ as well as the nonlinear dynamical systems approach by Ghidersa and Dušek⁵ have shown that azimuthal mode $m=1$ is the fastest growing. At this stage, no analysis has suggested that mode 2 might be the most important. It still might be possible, however, that a nonlinear and/or nonparallel stability analysis can predict the eventual dominance of mode 2, and as well explain the similarity between the eigenspectra presented here and those taken in the axisymmetric jet by Gamard *et al.*¹⁹

ACKNOWLEDGMENTS

One of us (W.K.G.) in 1968 joined John L. Lumley at the Pennsylvania State University, with the hope of initiating a POD study of the axisymmetric wake. Fate led our joint work there in other directions, but a fascination for Lumley's POD remained. Now, 33 years later, it is with no small measure of satisfaction that these results are presented for the first time at a symposium honoring John L. Lumley. They are offered both as tribute and thank you for his inspiration, as well as for his many contributions to science. This work was initially supported by the US Air Force Office of Scientific Research, Grant No. F49620-98-1-0143, and Chalmers University of Technology. It continues with the support of the Swedish Research Council, Grant No. 2641.

¹N. C. H. Hwang and L. V. Baldwin, "Decay of turbulence in axisymmetric wakes," *J. Basic Eng.* **88**, 261 (1966).

²E. Achenbach, "Vortex shedding from spheres," *J. Fluid Mech.* **62**, 209 (1974).

³A. I. Sirviente and V. C. Patel, "Experiment in the turbulent near wake of an axisymmetric body," *AIAA J.* **37**, 1670 (1999).

⁴P. A. Monkewitz, "A note on vortex shedding from axisymmetric bluff bodies," *J. Fluid Mech.* **192**, 561 (1988).

⁵B. Ghidersa and J. Dušek, "Breaking of axisymmetry and onset of unsteadiness in the wake of a sphere," *J. Fluid Mech.* **423**, 33 (2000).

⁶S. C. Cannon, Ph.D. thesis, University of Arizona, 1991.

⁷S. Cannon, F. Champagne, and A. Glezer, "Observations of large-scale structures in wakes behind axisymmetric bodies," *Exp. Fluids* **14**, 447 (1993).

⁸P. Johansson and W. K. George, "On the effect of finite Reynolds number and initial conditions on the axisymmetric wake," in *Turbulent Shear Flow Phenomena II*, Stockholm, 27–29 June 2001, Vol. 1, pp. 323–328.

⁹J. B. Roberts, "Coherence measurements in an axisymmetric wake," *AIAA J.* **11**, 1569 (1973).

¹⁰H. V. Fuchs, E. Mercker, and U. Michel, "Large scale coherent structures in the wake of axisymmetric bodies," *J. Fluid Mech.* **93**, 189 (1979).

¹¹E. Berger, D. Scholz, and M. Schumm, "Coherent vortex structures in the wake of a sphere and a circular disk at rest and under forced vibrations," *J. Fluids Struct.* **4**, 231 (1990).

¹²S. I. Lee and P. W. Bearman, "An experimental investigation of the wake structure behind a disk," *J. Fluids Struct.* **6**, 437 (1992).

¹³J. J. Miao, T. S. Leu, T. W. Liu, and J. H. Chou, "On vortex shedding behind a circular disk," *Exp. Fluids* **23**, 225 (1997).

¹⁴A. E. Perry and T. T. Lim, "Coherent structures in coflowing jets and wakes," *J. Fluid Mech.* **88**, 451 (1978).

¹⁵A. E. Perry and J. H. Watmuff, "The phase-averaged large-scale structures in three-dimensional turbulent wakes," *J. Fluid Mech.* **103**, 33 (1981).

¹⁶M. N. Glauser, Ph.D. thesis, State University of New York at Buffalo, 1987.

¹⁷M. N. Glauser and W. K. George, "Orthogonal decomposition of the axisymmetric jet mixing layer including azimuthal dependence," in *Advances in Turbulence*, edited by G. Comte-Bellot and J. Mathieu (Springer, Berlin, 1987), pp. 357–366.

¹⁸J. H. Citriniti and W. K. George, "Reconstruction of the global velocity field in the axisymmetric mixing layer utilizing the proper orthogonal decomposition," *J. Fluid Mech.* **418**, 137 (2000).

¹⁹S. Gamard, D. Jung, S. Woodward, and W. K. George, "Application of a 'slice' proper orthogonal decomposition to the far field of an axisymmetric turbulent jet," *Phys. Fluids* **14**, 2515 (2002).

²⁰M. N. Glauser and W. K. George, "Application of multipoint measurements for flow characterization," *Exp. Therm. Fluid Sci.* **5**, 617 (1992).

²¹J. L. Lumley, "The structure of inhomogeneous turbulent flows," in *Atmospheric Turbulence and Radio Wave Propagation*, edited by A. M. Yaglom and V. I. Tatarsky (Nauka, Moscow, 1967).

²²W. K. George, "Insight into the dynamics of coherent structures from a proper orthogonal decomposition," in *Symposium on Near Wall Turbulence*, Dubrovnik, Yugoslavia, 16–20 May 1988.

²³P. Holmes, J. L. Lumley, and G. Berkooz, *Turbulence, Coherent Structures, Symmetry and Dynamical Systems* (Cambridge University Press, Cambridge, 1996).

²⁴W. K. George, "Some thoughts on similarity, the POD, and finite boundaries," in *Trends in Mathematics*, edited by A. Gyr and A. Tsinober (Birkhauser, Basel, 1999), pp. 117–128.

²⁵J. L. Lumley, "On the interpretation of time spectra in high intensity shear flows," *Phys. Fluids* **8**, 1056 (1965).